PAPER

Experimental study of the magnetic characteristics of nanocrystalline thin films: the role of edge effects

View the article online for updates and enhancements.

Materials Research Express

Experimental study of the magnetic characteristics of nanocrystalline thin films: the role of edge effects

B A Belyaev[1,2], A V Izotov[1,2], G V Skomorokhov[1] and P N Solovev[1,2]

[1] Kirensky Institute of Physics, Federal Research Center KSC SB RAS, 50/38 Akademgorodok, Krasnoyarsk, 660036, Russia
[2] Siberian Federal University, 79 Svobodny pr., Krasnoyarsk, 66041, Russia
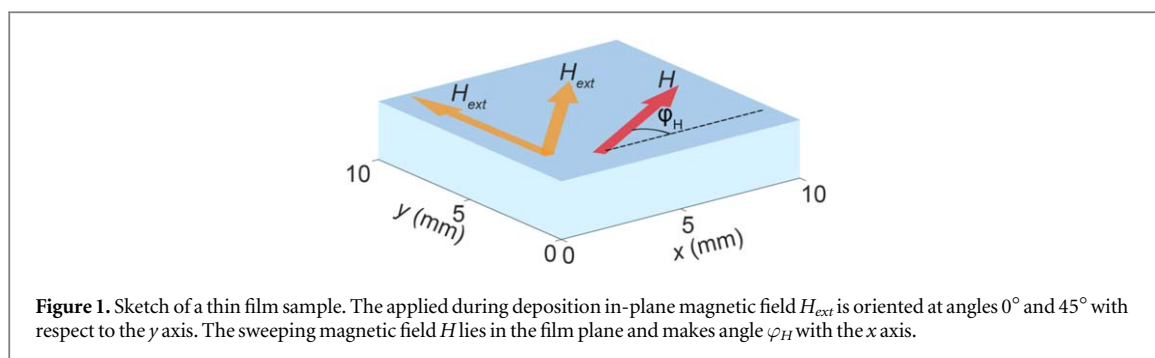
E-mail: psolovev@iph.krasn.ru

Abstract

Magnetic characteristics and their spatial distribution of magnetron sputtered nanocrystalline NiFe thin films of various compositions were investigated by ferromagnetic resonance (FMR) and magneto-optical Kerr effect microscopy. A sharp increase in the FMR linewidth and a strong deviation of the uniaxial magnetic anisotropy field were observed near the film edges. It was shown that the observed magnetic anisotropy behavior can be explained by assuming that besides the field-induced uniaxial magnetic anisotropy an additional source of the uniaxial anisotropy near the film edges exists, with the easy axis parallel to the edges. The possible origins of this additional contribution were discussed.

1. Introduction

Nanocrystalline magnetic thin films have gained a lot of attention over the last decades. This interest is mainly stimulated by the rapidly growing technological demand for magnetic materials with high magnetic susceptibility [1–3]. The excellent magnetic softness of nanocrystalline magnetic thin films stems from their microstructure. When the sizes of randomly oriented crystallites are smaller than the exchange length of the material the exchange energy starts dominating over the magnetocrystalline anisotropy energy. The local magnetocrystalline anisotropies are averaged out resulting in the very low coercivity [4] and the high magnetic susceptibility of the film [5, 6]. It is worth noting that these films demonstrate high susceptibility in a wide range from static to microwave magnetic fields, with the upper limit determined by the ferromagnetic resonance (FMR) frequency [2]. However, there is a number of factors that can lead to the formation of spatial variations of magnetic characteristics over the film area. Dispersion of the magnetic anisotropy, magnetization saturation, and other magnetic characteristics reduce the magnetic susceptibility [7, 8] and enhance the magnetic noise in a film. It was found that the magnetic noise caused by the spatial dispersion of the magnetic characteristics is the key factor that limits the sensitivity of the magnetic field sensors based on a thin magnetic film [9–11]. Usually, during deposition of thin magnetic films an external magnetic field is applied in the film plane. Under the influence of this field the uniaxial magnetic anisotropy is induced, mainly through the mechanism of atomic pair ordering for FeNi alloy films. The field 'smooths' nonuniformities of the magnetic microstructure, thereby reducing the dispersion of the film magnetic characteristics. However, edges of a film disturb its continuality and naturally lead to the nonuniformity of the magnetic characteristics in the vicinity of the film boundaries. These edge effects can have different origins. To minimize the magnetostatic energy magnetic moments near film edges may rearrange to spatially nonuniform configurations [12–14]. A film magnetized perpendicular to an edge and exited by a high-frequency magnetic field exhibits the localized 'edge modes' of the magnetization oscillations caused by the nonuniformity of an effective internal magnetic field at the film edges [15]. The symmetry breaking at the film edges leads to the formation of mechanical stresses gradients [16, 17] that through magnetostriction affect magnetic properties of the film [18, 19]. The film growth conditions near edges often differ from those in the central part [20–22], which may result in a non-uniform microstructure.

Figure 1. Sketch of a thin film sample. The applied during deposition in-plane magnetic field H_{ext} is oriented at angles 0° and 45° with respect to the y axis. The sweeping magnetic field H lies in the film plane and makes angle φ_H with the x axis.
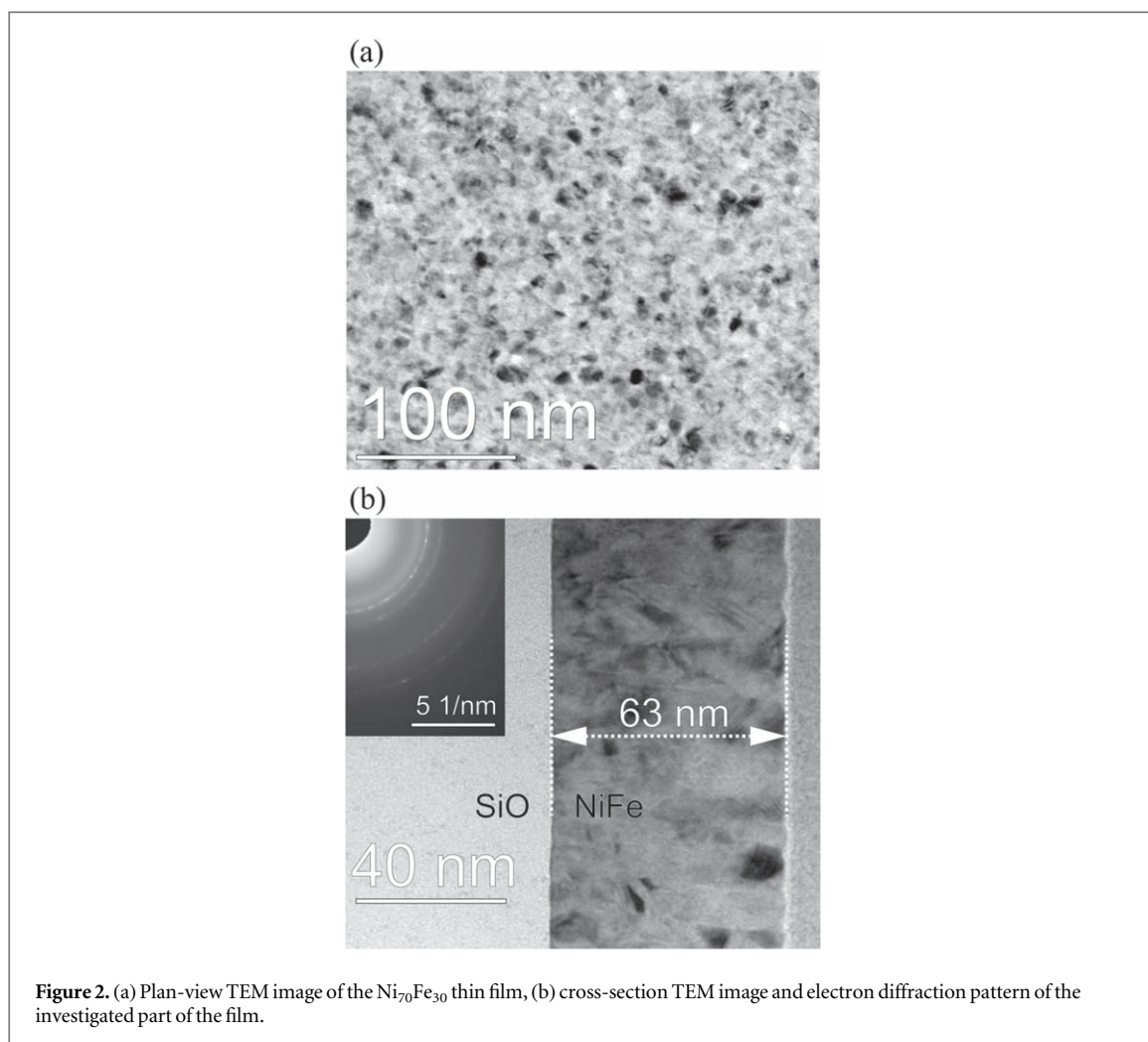
In this study, we experimentally investigated in detail the spatial variations in the magnetic properties of thin NiFe films of various compositions produced by magnetron sputtering with a focus on their edges. We found the sharp broadening of FMR linewidth and significant deviation of the uniaxial magnetic anisotropy parameters at the film edges compared to the central part. The possible reasons of the observed effects are discussed.

2. Experimental details

The investigated nanocrystalline magnetic thin films were produced by DC magnetron sputtering from high purity (99.95%) targets of the $Ni_{60}Fe_{40}$, $Ni_{70}Fe_{30}$, $Ni_{75}Fe_{25}$, $Ni_{80}Fe_{20}$, and $Ni_{85}Fe_{15}$ chemical compositions. The targets were discs 55 mm in diameter and with thickness of 2 mm. From each target five samples were produced (25 samples in total). The thin films were deposited on quartz glass 12 $\times$ 12 $\times$ 0.5 mm size square substrates with ~1 nm roughness. To exclude the possibility of large crystallites formation on the initial stage of film growth due to epitaxy the substrates were preliminary covered by SiO layer with thickness of 500 nm. The substrates were placed in the substrate holder with a square mask 10 $\times$ 10 mm size. The distance between the target and the substrate during film deposition was 170 mm. The power density at the magnetron was kept constant at 11 W cm^{-2}, which provideda deposition rate of 0.25 nm s^{-1}. The base pressure was 3 $\times$ 10^{-4} Pa while Ar pressure was 2 $\times$ 10^{-1} Pa. The thickness of each thin magnetic film was ≈60 nm. During the deposition process, substrates temperature of 200 °C was maintained, and an orienting external magnetic field $H_{ext} = 200$ Oe was applied in the film plane. For all the samples, except one, the magnetic field H_{ext} was parallel to one edge of the substrate (the y axis). A special deposition was performed, where two $Ni_{80}Fe_{20}$ samples were simultaneously produced during one sputtering, with the y axis oriented at 0° for the first sample and at 45° for the second sample with respect to the field H_{ext} (figure 1).

The chemical composition of the films was determined by an x-ray fluorescence analysis (spectrometer S4 Pioneer, Bruker). It showed that, on average, the composition of films differed from that of the targets by less than 1.5 wt %. The transmission electron microscopy (TEM, Hitachi HT-7700) revealed that our samples had a nanocrystalline microstructure, with the crystallites sizes of about 4-10 nm (see figure 2(a)). The cross-section TEM of the samples confirms the low roughness of the substrates and also shows that the films thickness differs from the nominal thickness by no more that 5% (figure 2(b)). The electron diffraction pattern of the investigated part of the film is typical of a polycrystalline material. The observed reflections correspond to a face-centered cubic structure (fm-3m space group).

The magnetic properties of the samples were analyzed by the FMR spectrometry and magneto-optical Kerr effect (MOKE) microscopy. Ferromagnetic resonance is one of the most informative and accurate techniques of measuring thin films magnetic characteristics [23–25]. FMR measurements were performed using the scanning FMR spectrometer. The spectrometer's design, peculiarities of its usage, and its operational characteristics were described in detail in ref. [26]. Briefly, in the spectrometer, the microstrip resonator fabricated on a dielectric substrate was used as a sensor. Because of the small volume of the microstrip resonator, the spectrometer is highly sensitive even in the decimeter wave band thus providing an opportunity to study effects on local areas of thin films that is hard to detect in large magnetic fields. The measuring hole was etched in the ground plane of the resonator near the antinode of high-frequency magnetic field. The hole diameter (~1 mm) determined the locality of measurements. The FMR measurements were performed across the sample with a step of 1 mm. The microwave pump frequency was 2.3 GHz. The resonance field (field at a point where the differential FMR curve changes sign) was determined with an accuracy of 0.05 Oe, and the peak-to-peak linewidth was determined with an accuracy of 0.1 Oe. The uniaxial in-plane magnetic anisotropy of the films was retrieved from the experimental angular dependences of the resonance field by fitting the parameters of a theoretical model of a single-domain film to the experimental data [27, 28].

Figure 2. (a) Plan-view TEM image of the $Ni_{70}Fe_{30}$ thin film, (b) cross-section TEM image and electron diffraction pattern of the investigated part of the film.

A few samples were also investigated by MOKE microscopy (NanoMOKE2, Durham Magneto Optics Ltd). The light source was a current and temperature stabilized solid state laser with an operating wavelength of 630-640 nm and an output power of 2.5 mW. The accurate determination of the magnetic anisotropy parameters from the Kerr measurements is not a trivial task [29]. We used a simplified approach for the qualitative analysis of the samples. For a thin magnetic film with a uniaxial anisotropy in a single-domain state the slope of the linear part of the hysteresis loop $M_H(H)$ obtained in in-plane field H applied along the hard axis is inversely proportional to the uniaxial magnetic anisotropy field. Therefore, we calculated the dH/dM_H ratio from MOKE hysteresis loops (where the in-plane magnetic field H is directed along the hard axis, and M_H is the normalized magnetization), which allowed us to investigate the relative distribution of the uniaxial magnetic anisotropy field over the films surfaces.

3. Results and discussion

Figure 3 shows typical differential absorption FMR curves measured by the scanning FMR spectrometer. The presented curves were obtained along the easy and hard axes of magnetization on two local areas of the $Ni_{75}Fe_{25}$ film — in its center, and near one of the edges. A relative decrease in the FMR signal amplitude near the film edge is related to the fact that, in this case, the investigated area of the film did not completely cover the measuring hole of the microstrip resonator. In all the measurements, only absorption peaks corresponding to the uniform FMR mode were observed in the spectra measured while sweeping the magnetic field over the available range of 0–300 Oe. Figure 4 shows the obtained from the measured spectra dependences of the resonance field H_R and FMR linewidth ΔH on the sweeping field direction φ_H for the $Ni_{75}Fe_{25}$ film measured on its two local areas. These angular dependences demonstrate that the film has a uniaxial in-plane magnetic anisotropy with the easy axis parallel to the y axis. It can be also seen that the anisotropy field in the film center is slightly less than the anisotropy field near the film edge that is parallel to the y axis.
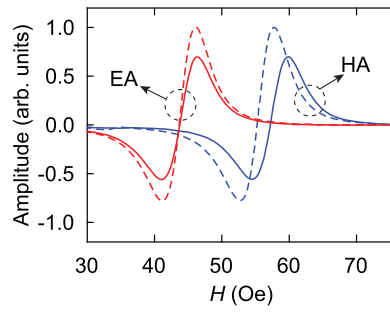
Figure 3. Differential absorption FMR curves measured along the easy axis (EA, red lines) and hard axis (HA, blue lines) of magnetization for the $Ni_{75}Fe_{25}$ film on its two local areas: $x = 5$ mm, $y = 5$ mm (dashed lines), and $x = 0$ mm, $y = 5$ mm (solid lines).

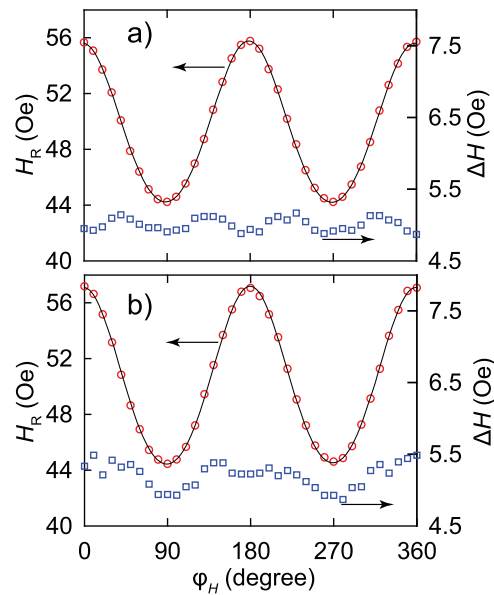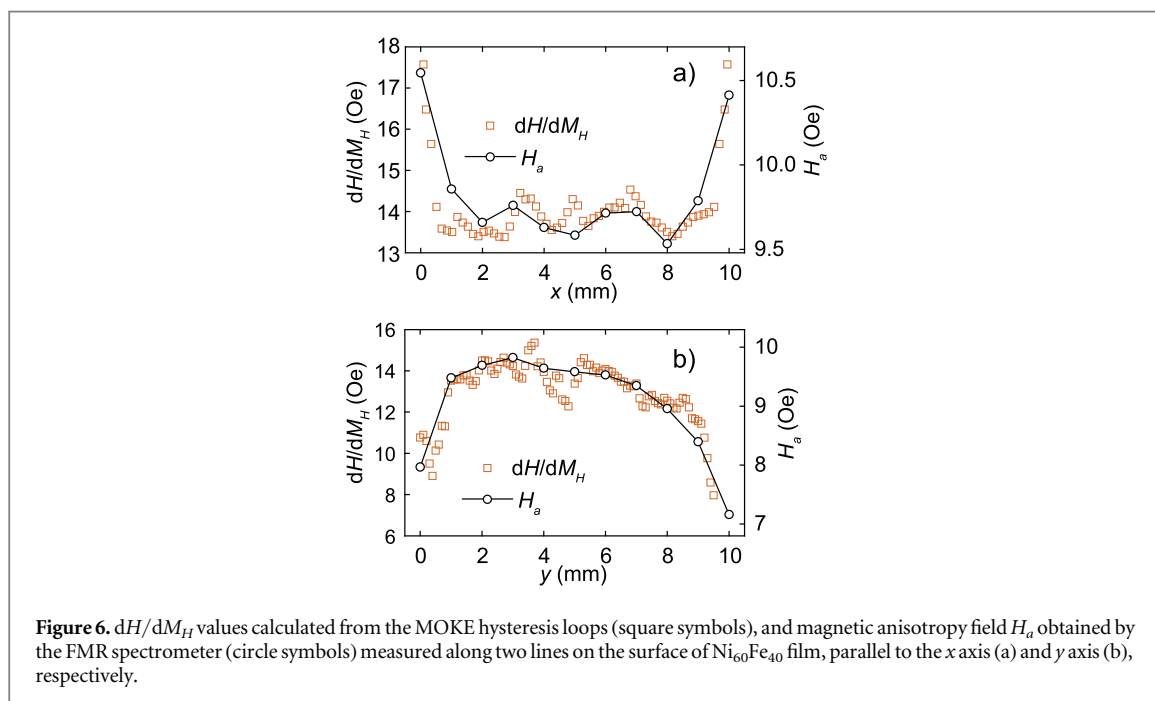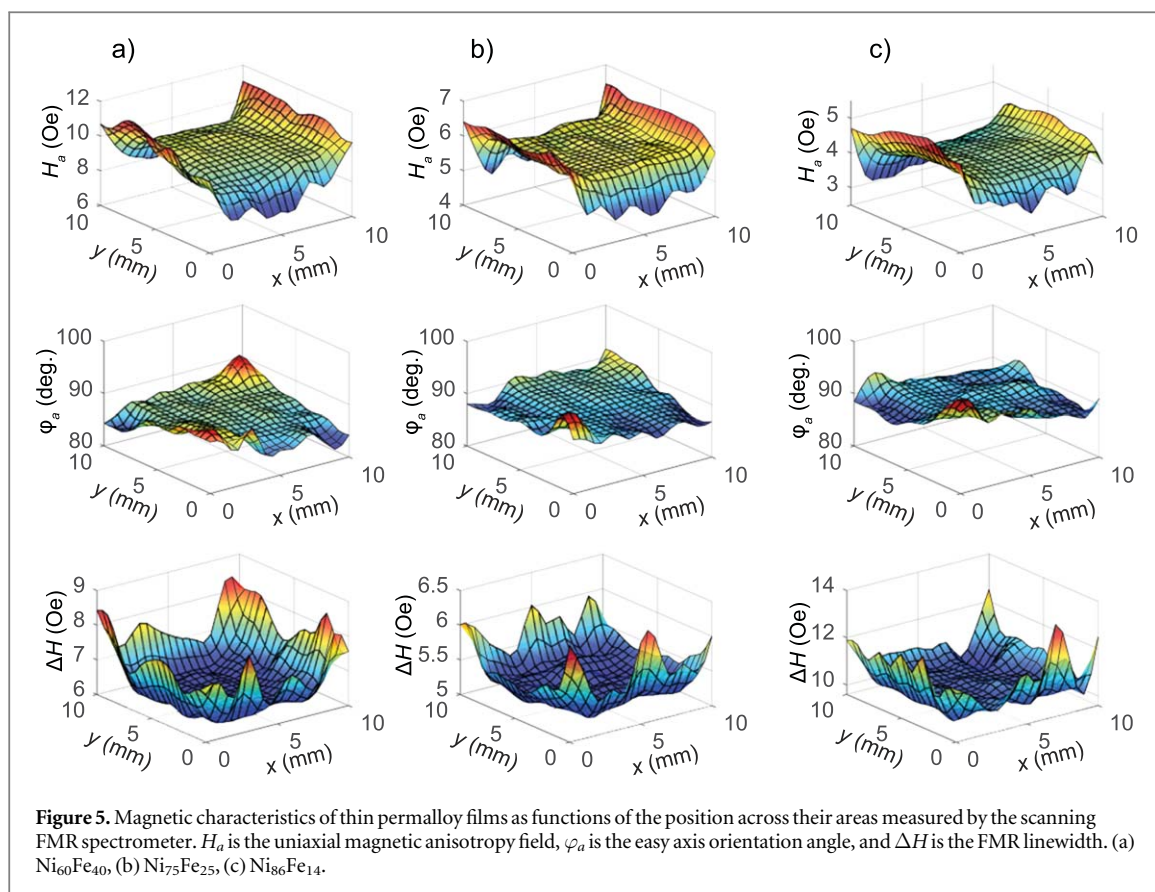**Figure 4.** Dependences of the resonance field H_R and FMR linewidth ΔH on the sweeping field direction φ_H for the $Ni_{75}Fe_{25}$ film measured on its two local areas: (a) $x = 5$ mm, $y = 5$ mm, (b) $x = 0$ mm, $y = 5$ mm. Symbols correspond to the experimental results, while lines are theoretical fits.

With the help of the scanning FMR spectrometer, we measured the magnetic characteristics of all the samples as functions of the position across their areas. Figure 5 shows the results for thin films of three compositions. Note that these surfaces were drawn using the smoothed experimental data for better visibility of spatial nonuniformities. Here, a relatively high uniformity of the spatial distribution of the magnetic characteristics in the central part of

the film is abruptly disturbed at the edges. The most interesting features are a sharp increase in the FMR linewidth ΔH and a strong deviation of the uniaxial magnetic anisotropy field H_a at the film edges. In the vicinity of the edges parallel to the magnetic field H_{ext} applied during film deposition (parallel to the y axis), the anisotropy field H_a is about 25% greater than H_a in the central part while H_a near edges perpendicular to H_{ext} (parallel to the x axis) is weaker by approximately the same value. The standard deviation (std) of the anisotropy field calculated across the film area excluding edges (1 mm away from the edges) is about four times less than the std for the whole film area. A similar picture can be seen in the FMR linewidth distribution with the exception that the ΔH value increases near all the edges independent of their orientation with respect to the field H_{ext}. On the contrary, the distribution of the easy axis orientation angle φ_a (measured with respect to the x axis) has no features near the film edges and, in general, the easy axis follows the direction of the field H_{ext}.

The results of MOKE and FMR measurements of the $Ni_{60}Fe_{40}$ sample are shown in figure 6. The MOKE measurements with a step of 0.1 mm were performed along two lines on the film surface, which were parallel to the x and y axis, respectively, and crossed at the center of the film. Square symbols in figure 6 correspond to dH/dM_H values calculated from MOKE hysteresis loops (figure 7 as an example) and circle symbols connected by a line represent the magnetic anisotropy field H_a obtained by the FMR spectrometer at the same local areas of

Figure 5. Magnetic characteristics of thin permalloy films as functions of the position across their areas measured by the scanning FMR spectrometer. H_a is the uniaxial magnetic anisotropy field, φ_a is the easy axis orientation angle, and ΔH is the FMR linewidth. (a) $Ni_{60}Fe_{40}$, (b) $Ni_{75}Fe_{25}$, (c) $Ni_{86}Fe_{14}$.

Figure 6. dH/dM_H values calculated from the MOKE hysteresis loops (square symbols), and magnetic anisotropy field H_a obtained by the FMR spectrometer (circle symbols) measured along two lines on the surface of $Ni_{60}Fe_{40}$ film, parallel to the x axis (a) and y axis (b), respectively.

the film but with a step of 1 mm. There is a good qualitative correspondence between results obtained by two different magnetometry methods, although the MOKE signal seems much noisier than the FMR one. This may be attributed to the fact that the MOKE microscopy probes only a small fraction of the film volume as it has a very high spatial locality (the laser spot is $\sim$5 μm in diameter) and light penetrates into the film only $\sim$25 nm deep [30]. The scanning FMR spectrometer measures magnetic parameters of the much larger film volume (surface region of $\sim$1 mm in diameter and over the entire film thickness) averaging magnetic nonuniformities that results in smoother dependencies. The high spatial resolution of the MOKE microscopy allows us to
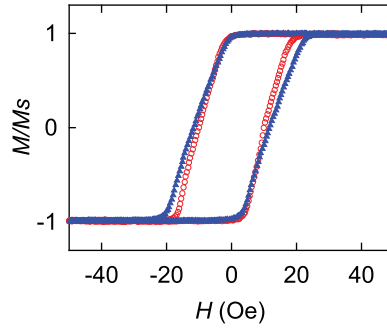
Figure 7. MOKE hysteresis loops measured along the hard axis of magnetization at two points of the $Ni_{60}Fe_{40}$ film: $x = 5$ mm, $y = 5$ mm (open symbols), and $x = 0$ mm, $y = 5$ mm (filled symbols).
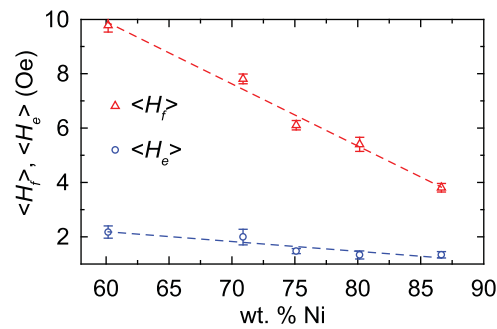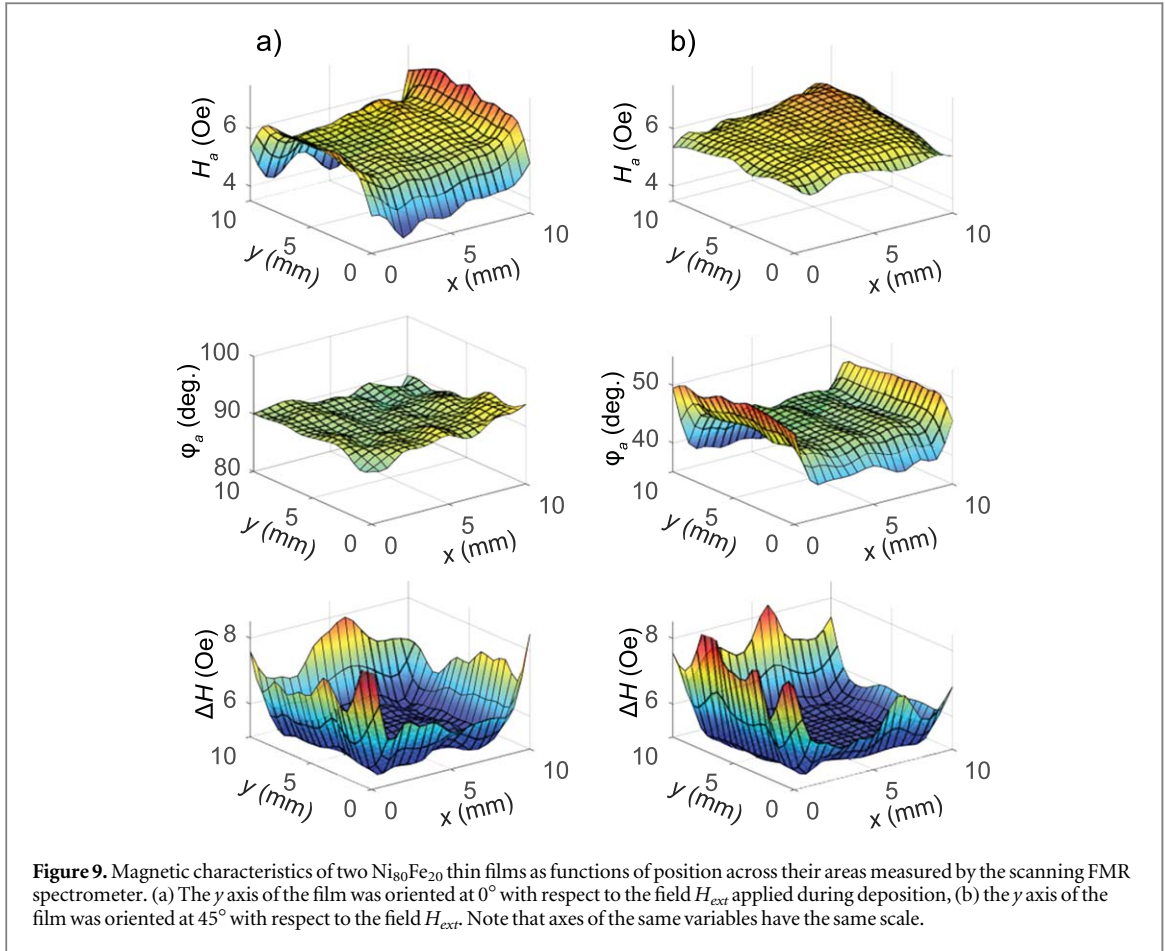

Figure 8. Dependences of the averaged magnetic anisotropy fields $\langle H_f \rangle$ and $\langle H_e \rangle$ (see text) on nickel concentration. Dashed lines are linear fits.

consider closely the magnetic behavior near the film edges. It reveals that the dH/dM_H deviation decreases with increasing distance from the edges not abruptly but rather monotonically and vanishes at a distance of about 1 mm away from the edges for all sides of the sample.

In general, it was found that for all the investigated films the magnetic anisotropy behavior at the opposite edges is almost symmetrical and the positive deviation of H_a from the mean value approximately equals to the negative one. Moreover, as expected, the magnetic anisotropy fields depend on the chemical composition of the films. Hence, it is of interest to investigate both the behavior of the averaged magnetic anisotropy $\langle H_f \rangle$ of

each sample without consideration of edge effects (1 mm away from the edges) and the behavior of the contribution of the edge effects themselves as a function of the nickel concentration. The contribution of the edge effects was estimated by the averaged value $\langle H_e \rangle$ determined as an absolute difference between the mean anisotropy fields H_a measured on each pair of the opposite edges and $\langle H_f \rangle$. We can consider $\langle H_f \rangle$ as the averaged field of the uniaxial magnetic anisotropy induced by the magnetic field applied during deposition (the field-induced anisotropy), and $\langle H_e \rangle$ as the averaged field of the additional magnetic anisotropy induced near the film edges.

The obtained dependences are given in figure 8, where error bars indicate the standard deviation. It can be seen that the magnetic anisotropy field $\langle H_f \rangle$ drops linearly with an increase in the nickel concentration from 60 to 86 wt %. This accurately reproduces the well-known results of the study on NiFe films that were explained by the theory of atomic pair ordering under the magnetic field applied during film deposition [31, 32]. $\langle H_e \rangle$ also exhibits a linear dependence on the composition, decreasing from 2.17 Oe at 60 wt % of Ni to 1.3 Oe at 86 wt % of Ni. It is important to note that for the films of all compositions the symmetry of the magnetic anisotropy field distribution is the same (figure 5).

The observed features in the anisotropy field behavior can be explained if we assume that a mechanism exists that induces an additional contribution to the uniaxial magnetic anisotropy near the film edges, with the easy axis parallel to the edges. Indeed, let us consider two uniaxial magnetic anisotropies: the anisotropy formed by a magnetic field applied during deposition with the field H_f, and the anisotropy induced near the film edges with the field H_e. In this case, the energy of the measured uniaxial magnetic anisotropy $F_a = -\frac{H_a M_s}{2} \cos^2(\varphi_M - \varphi_a)$ is the sum of the energy of the anisotropy induced by the magnetic field $F_f = -\frac{H_f M_s}{2} \cos^2(\varphi_M - \varphi_f)$ and the energy of the anisotropy induced near the edges $F_e = -\frac{H_e M_s}{2} \cos^2(\varphi_M - \varphi_e)$. Here M_s is the saturation

Figure 9. Magnetic characteristics of two $Ni_{80}Fe_{20}$ thin films as functions of position across their areas measured by the scanning FMR spectrometer. (a) The *y* axis of the film was oriented at 0° with respect to the field H_{ext} applied during deposition, (b) the *y* axis of the film was oriented at 45° with respect to the field H_{ext}. Note that axes of the same variables have the same scale.

magnetization of the film, φ_M is the angle of the equilibrium position of magnetization, φ_f and φ_e are the angles that determine easy axes directions of anisotropies H_f and H_e, respectively. This results in the following system of equations [33]

$$
\begin{cases}
H_a \cos 2(\varphi_M - \varphi_a) = H_f \cos 2(\varphi_M - \varphi_f) \\
\qquad\qquad\qquad\qquad + H_e \cos 2(\varphi_M - \varphi_e) \\
H_a \sin 2(\varphi_M - \varphi_a) = H_f \sin 2(\varphi_M - \varphi_f) \\
\qquad\qquad\qquad\qquad + H_e \sin 2(\varphi_M - \varphi_e)
\end{cases}
\tag{1}
$$

from which we can determine the value and orientation angle of the experimentally observed uniaxial magnetic anisotropy

$$
H_a = \sqrt{H_f^2 + H_e^2 + 2H_f H_e \cos 2(\varphi_f - \varphi_e)},
$$
$$
\varphi_a = \frac{1}{2}\left[\varphi_f + \varphi_e + \text{atan}\left(\frac{H_f - H_e}{H_f + H_e}\tan(\varphi_f - \varphi_e)\right)\right].
\tag{2}
$$

Assuming $H_f \rangle H_e$, from equation (2) follows that if the easy axes of the two anisotropies are parallel (orthogonal) then the resulting anisotropy field simply equals to the sum (difference) of the two anisotropy fields, and the orientation angle of the resulting easy axis equals to φ_f. This corresponds to the observed behavior of the magnetic anisotropy shown in figure 5.

However, in the general case of arbitrary orientations of the two easy axes the easy axis of the resulting uniaxial anisotropy should be somewhere in between those two. To confirm this, we fabricated two $Ni_{80}Fe_{20}$ samples obtained by simultaneous deposition on the two substrates whose *y* axes were oriented at 0° and 45° with respect to the magnetic field H_{ext} applied during deposition. The distribution of the magnetic characteristics across the films area measured by the scanning FMR spectrometer are shown in figure 9. Additionally, figure 10 shows the easy axis distributions plotted using the data presented in figure 9, but where the axis deviation from the direction of the field H_{ext} was enlarged by a factor of six to make it clearly visible. It can be seen that in the film oriented at ±45° with respect to H_{ext} the easy axis is tilted toward the edges. For the film whose magnetic characteristics are presented in figure 9(a), where the average H_a fields at the adjacent edges

Figure 10. Easy axis distributions in the two $Ni_{80}Fe_{20}$ samples, with the *y* axis oriented at 0° (a) and 45° (b) with respect to the field H_{ext} applied during deposition. The easy axis deviation from the H_{ext} direction is enlarged by a factor of six.
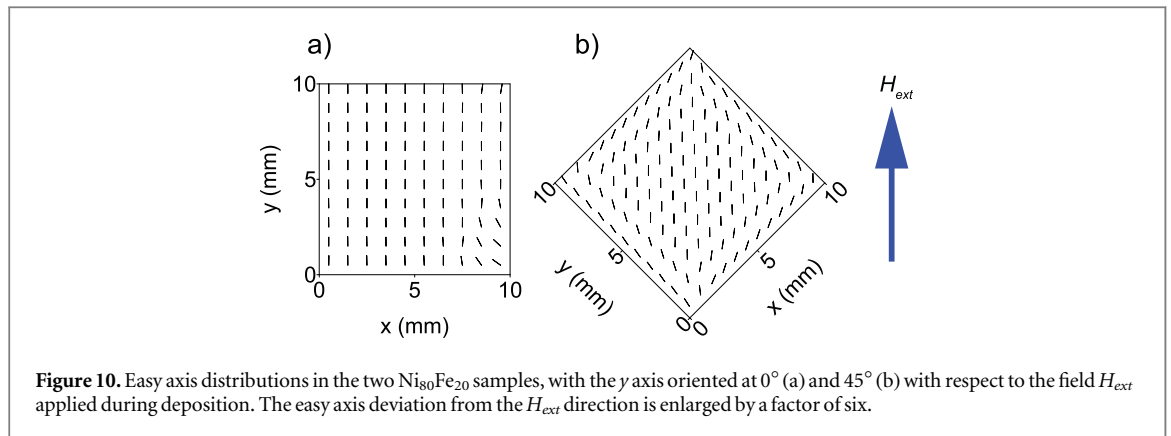
equals 6.7 Oe and 4.3 Oe, respectively, $\varphi_e = 90°$ and 0°, $\varphi_f = 90°$, we can assume that $H_f = \langle H_f \rangle = 5.9$ Oe and $H_e = \langle H_e \rangle = 1.2$ Oe. For these two values of the anisotropy fields and angles $\varphi_f = 90°$ and $\varphi_e = 45°$ equation (2) gives us $H_a = 6.02$ Oe, $\varphi_a = 84.3°$. The calculated orientation angle deviation from H_{ext} of the resulting anisotropy (5.7°) is very close to the measured average easy axis orientation angle deviation from H_{ext} (5.5°) at the edges of the film oriented at $\pm45°$ with respect to H_{ext} (figure 9(b)), while the calculated H_a value only slightly differs from H_f that is also in good agreement with the experiment.

This confirms that in our samples near the edges an additional contribution to the energy of the uniaxial magnetic anisotropy exists. The field of this additional magnetic anisotropy approximately equals to the $\langle H_e \rangle$ value measured for the films deposited in a magnetic field oriented along one of their edge. It is interesting to note that a similar effect was observed in thin sputtered FeSi films during investigation of their magnetic domains structure [34]. It was found that near the film edges the magnetization tends to align parallel to the edges. The authors attributed this behavior to the uniaxial magnetic anisotropy of unclear origin formed near the film edges.

The dependence of $\langle H_e \rangle$ on the composition (figure 8) suggests that mechanical stresses can contribute to the energy of this additional anisotropy formed near the edges but they cannot be the sole source of $\langle H_e \rangle$, otherwise for $Ni_{86}Fe_{14}$ film the easy axis of the additional anisotropy should rotate by 90° as the magnetostriction constant changes sign at $Ni_{82}Fe_{18}$ [35], which contradicts the experiment (figure 5(c)). However, it is possible that during film growth an inhomogeneous morphology of anisotropic character in the microcrystalline structure forms near the film edges. This may be caused by a temperature gradient during sputtering or by influence of the edges of the substrate holder on the angle and energy distribution of deposited particles. Because of the dipolar interaction, these anisotropic structural irregularities are the source of additional contribution to the magnetic anisotropy energy. This assumption is supported by the behavior of the FMR linewidth (figures 5 and 9). The broadening of the FMR line in polycrystalline thin magnetic films is mainly attributed to the extrinsic magnetic relaxation processes [36]. The inhomogeneous effective magnetic field provides interactions between spin-wave modes that allow the energy of the uniform magnetization oscillation to transfer to the other normal oscillation modes resulting in an additional damping of the uniform mode [37]. Therefore, the observed sharp broadening of the FMR line at the film edges indicates the increase in inhomogeneity of the effective magnetic field most probably caused by the increase of structural irregularities in the vicinity of the film edges.

4. Conclusion

In this paper, the magnetic characteristics and their spatial nonuniformity of DC magnetron sputtered nanocrystalline NiFe thin films were investigated by means of the FMR spectrometry and MOKE microscopy. A sharp increase in the FMR linewidth and strong deviation of the uniaxial magnetic anisotropy field from its average value were observed near the film edges. These edge effects monotonically decline with increasing distance from the edges and vanish at a distance of ~1 mm away from the edges. It was shown that the observed magnetic anisotropy behavior can be explained by assuming that in addition to the field-induced uniaxial magnetic anisotropy another source of uniaxial anisotropy near the film edges exists, with the easy axis parallel to the edges. The field of this additional anisotropy is about 25% of the field-induced anisotropy field. The dependence of the magnetic anisotropy field on the nickel concentration suggests that this additional contribution to the anisotropy energy cannot be solely attributed to mechanical stresses. It is possible that the anisotropic structural irregularities formed during the growth near the film edges are the source of the additional contribution to the magnetic anisotropy. The presence of these irregularities explains the observed broadening of the FMR line near the edges.

It is important for application that the observed edge effects increase the dispersion of uniaxial anisotropy value for the entire film up to four times. The obtained results can be used in designing devices based on thin magnetic films. Particularly, in the study we provided absolute values of this effect for the permalloy films of different compositions thus giving information for practitioners whether the extra efforts are needed for mitigating these edge effects in their specific cases.

Acknowledgments

ORCID iDs

P N Solovev ● https://orcid.org/0000-0003-3545-7599

References

[1] Petzold J 2002 *J. Magn. Magn. Mater.* **242–245** 84–9
[2] Lagarkov A N and Rozanov K N 2009 *J. Magn. Magn. Mater.* **321** 2082–92
[3] Yamaguchi M, Hyeon Kim K and Ikedaa S 2006 *J. Magn. Magn. Mater.* **304** 208–13
[4] Belyaev B A, Izotov A V and Leksikov A A 2010 *Phys. Solid State* **52** 1664–72
[5] Herzer G 1996 *J. Magn. Magn. Mater.* **157/158** 133–6
[6] Herzer G 1995 *Scr. Metall. Mater.* **33** 1741–56
[7] Belyaev B A, Izotov A V and Kiparisov S Y 2001 *J. Exp. Theor. Phys. Lett.* **74** 226–30
[8] Craus C B, Palasantzas G, Chezan A R, De Hosson J, Th M, Boerma D O and Niesen L 2005 *J. Appl. Phys.* **97** 013904
[9] Tumański S 2001 *Thin Film Magnetoresistive Sensors* (Bristol and Philadelphia: Institute of Physics Publishing)
[10] Babitskii A N, Belyaev B A, Boev N M, Skomorokhov G V, Izotov A V and Galeev R G 2016 *Instrum. Exp. Tech.* **59** 425–32
[11] Belyaev B A, Boev N M, Izotov A V, Solovyev P N and Tyurnev V V 2018 *Russ. Phys. J.* **61** 1367–75
[12] Deak J G and Koch R H 2000 *J. Magn. Magn. Mater.* **213** 25–31
[13] Bryan M T, Atkinson D and Cowburn R P 2004 *Appl. Phys. Lett.* **85** 3510–2
[14] Herrmann M, McVitie S and Chapman J N 2000 *J. Appl. Phys.* **87** 2994–9
[15] Maranville B B, McMichael R D, Kim S A, Johnson W L, Ross C A and Cheng J Y 2006 *J. Appl. Phys.* **99** 08C703
[16] Hoffman R W 1981 *Surf. Interface Anal.* **3** 62–6
[17] Murray C E 2006 *J. Appl. Phys.* **100** 103532
[18] McCord J 2004 *J. Appl. Phys.* **95** 6855–7
[19] Wenisch J, Gould C, Ebel L, Storz J, Pappert K, Schmidt M J, Kumpf C, Schmidt G, Brunner K and Molenkamp L W 2007 *Phys. Rev. Lett.* **99**
[20] Luo J K, Chu D P, Flewitt A J, Spearing S M, Fleck N A and Milne W I 2005 *J. Electrochem. Soc.* **152** C36
[21] Glathe S, Zeisberger M, Mattheis R and Hesse D 2010 *Appl. Phys. Lett.* **97** 112508
[22] Maranville B B, McMichael R D and Abraham D W 2007 *Appl. Phys. Lett.* **90** 232504
[23] Maksymov I S and Kostylev M 2015 *Phys. E* **69** 253–93
[24] Silva E F *et al* 2017 *J. Phys. D: Appl. Phys.* **50** 185001
[25] Cao D *et al* 2018 *J. Phys. D: Appl. Phys.* **51** 025001
[26] Belyaev B A, Izotov A V and Leksikov A A 2005 *IEEE Sens. J* **5** 260–7
[27] Belyaev B A, Izotov A V and Solovev P N 2016 *Phys. B Condens. Matter* **481** 86–90
[28] Belyaev B A, Izotov A V, Solovev P N and Yakovlev I A 2017 *J. Magn. Magn. Mater.* **440** 181–4
[29] Berling D, Zabrocki S, Stephan R, Garreau G, Bubendorff J L, Mehdaoui A, Bolmont D, Wetzel P, Pirri C and Gewinner G 2006 *J. Magn. Magn. Mater.* **297** 118–40
[30] Qiu Z Q and Bader S D 2000 *Rev. Sci. Instrum.* **71** 1243–55
[31] Smith D O 1959 *J. Appl. Phys.* **30** S264–5
[32] Han-Min J, Kim C-O, Lee T-D and Kim H-J 2007 *Chin. Phys.* **16** 3520–35
[33] Belyaev B A and Izotov A V 2007 *Phys. Solid State* **49** 1731–9
[34] Pockrand I and Verweel J 1975 *Phys. Status Solidi* A **27** 413–27
[35] Klokholm E and Aboaf J A 1981 *J. Appl. Phys.* **52** 2474–6
[36] Sparks M 1970 *Phys. Rev.* B **1** 3856–69
[37] McMichael R D and Krivosik P 2004 *IEEE Trans. Magn.* **40** 2–11